THE JOURNAL OF BIOLOGICAL CHEMISTRY Vol. 279, No. 3, Issue of January 16, pp. 2109–2116, 2004
Printed in U.S.A.

The Parathyroid Hormone mRNA 3′-Untranslated Region AU-rich Element Is an Unstructured Functional Element*

Received for publication, May 20, 2003, and in revised form, September 17, 2003
Published, JBC Papers in Press, October 29, 2003, DOI 10.1074/jbc.M305302200

Rachel Kilav, Osnat Bell, Shu-Yun Le‡, Justin Silver, and Tally Naveh-Many§

From the Minerva Center for Calcium and Bone Metabolism, Nephrology Services, Hadassah Hospital, The Hebrew University Medical School, P.O. Box 12000, Jerusalem, Israel 91120 and ‡Laboratory of Experimental and Computational Biology, NCI-Frederick Center for Cancer Research, National Institutes of Health, Frederick, Maryland 21702

Parathyroid hormone (PTH) gene expression is regulated post-transcriptionally by hypocalcemia and hypophosphatemia. This regulation is dependent upon binding of protective *trans*-acting factors to a specific element in the PTH mRNA 3′-untranslated region (UTR). We have previously demonstrated that a 63-nucleotide (nt) AU-rich PTH mRNA element is sufficient to confer regulation of RNA stability by calcium and phosphate in an *in vitro* degradation assay (IVDA). The 63-nt element consists of a core 26-nt minimal binding sequence and flanking regions. We have now studied the functionality of this element in HEK293 cells using reporter genes and showed that it destabilizes mRNAs for green fluorescent protein (GFP) and growth hormone, similar to its effect in the IVDA. To understand how the *cis*-element functions as an instability element, we have analyzed its structure by RNase H, primer extension, and computer modeling. The results indicate that the PTH mRNA 3′-UTR and in particular the region of the *cis*-element are dominated by significant open regions with little folded base pairing. Mutation analysis of the 26-nt core element demonstrated the importance of defined nucleotides for protein-RNA binding. In the GFP reporter system, the same mutations that prevented binding were also ineffective in destabilizing GFP mRNA in HEK293 cells. This is the first study of an AU-rich element that relates function to structure. The PTH mRNA 3′-UTR *cis*-acting element is an open region that utilizes the distinct sequence pattern to determine mRNA stability by its interaction with *trans*-acting factors.

PTH[1] has a central role in maintaining normal calcium and phosphate homeostasis as well as bone strength. The parathyroids (PTs) are regulated by calcium, phosphate, and $1,25(OH)_2$ vitamin D_3 (1). Hypocalcemia dramatically increases PTH mRNA levels, secretion, and, after prolonged stimulation, PT cell proliferation (2). The increase in PTH mRNA levels is post-transcriptional. Phosphate also regulates PTH secretion, gene expression, and PT cell proliferation (3, 4). Dietary induced phosphate depletion dramatically decreases PTH mRNA levels, and this is also post-transcriptional (3). We have shown that this post-transcriptional regulation is mediated by protein-RNA interactions involving protein binding to a specific element in the PTH mRNA 3′-UTR that determine PTH mRNA stability (2, 5). Protein binding to the PTH mRNA 3′-UTR was increased by hypocalcemia and decreased by hypophosphatemia. The regulation of binding by calcium and phosphate was observed only in the PT and not in other tissues of the same rats. We have identified AUF1 (heterogeneous nuclear ribonucleoprotein D) as a protein *trans*-acting factor that stabilizes the PTH mRNA (6). There is no PT cell line; therefore, we have utilized a cell-free mRNA *in vitro* degradation assay (IVDA) to demonstrate the functionality of the parathyroid cytosolic proteins in determining the stability of the PTH transcript. This assay has been shown to authentically reproduce cellular decay processes. PT protein extracts from hypocalcemic rats stabilized and PT protein extracts from hypophosphatemic rats destabilized the full-length PTH transcript, correlating with mRNA levels *in vivo*. Deletion of the protein-binding element of the PTH mRNA 3′-UTR resulted in stabilization of the transcript compared with the full-length PTH transcript. Moreover, calcium and phosphate did not regulate the stability of the truncated transcript. Therefore, the IVDA reproduces the *in vivo* stabilizing effect of low calcium and destabilizing effects of low phosphate on PTH mRNA levels, and this regulation in the IVDA is dependent upon protein binding that protects an instability sequence in the PTH mRNA 3′-UTR (2). However, it is not known yet if the PTH mRNA 3′-UTR protein-binding element is the cleavage site itself or if it induces some exonucleolytic pathway that acts either on the 5′ or the 3′-end of the mRNA.

We have identified the minimal sequence for protein binding in the PTH mRNA 3′-UTR and determined its functionality. A minimal sequence of 26 nt in the PTH mRNA 3′-UTR was sufficient for protein binding. To study the functionality of the protein binding element in the context of a different RNA, a 63-bp fragment coding for the 26 nt and flanking nt was fused to growth hormone (GH) reporter gene. RNAs were transcribed *in vitro*, and transcripts were subjected to IVDA with PT proteins. The chimeric GH PTH 63-nt transcript, as the full-length PTH transcript, was stabilized by PT proteins from rats fed a low calcium diet and destabilized by proteins of a low phosphate diet, correlating with PTH mRNA levels *in vivo*. The native GH transcript was more stable than PTH and the chimeric RNAs and was not affected by PT proteins from the different diets. These results demonstrate that the protein binding region of the PTH mRNA 3′-UTR is both necessary and sufficient to confer responsiveness to calcium and phosphate and determines PTH mRNA stability and levels (5).

* This work was supported in part by grants from the Israel Academy of Sciences, the U.S.-Israel Binational Foundation, the Hadassah research fund for women's health (to T. N.-M.), and the Minerva Foundation. The costs of publication of this article were defrayed in part by the payment of page charges. This article must therefore be hereby marked "*advertisement*" in accordance with 18 U.S.C. Section 1734 solely to indicate this fact.

§ To whom correspondence should be addressed. Tel.: 972-2-6776789; Fax: 972-2-6421234; E-mail: tally@huji.ac.il.

[1] The abbreviations used are: PTH, parathyroid hormone; PT, parathyroid(s); IVDA, *in vitro* degradation assay; UTR, untranslated region; GFP, green fluorescent protein; SIGSCR, significance score; STBSCR, stability score; nt, nucleotide(s); WT, wild type; REMSA, RNA electrophoretic mobility shift assay; ARE, AU-rich element; DRB, 5,6-dichloro-1-β-D-ribofuranosylbenzimidazole.

We have now studied the function of the PTH element in cells, using the heterologous cell line HEK293. Plasmids containing the native GH or GFP gene or chimeric genes containing the PTH 3′-UTR sequences at the 3′-end of the gene were transiently transfected into HEK293 cells, and mRNA levels were measured by Northern blot. There was a marked decrease in GH and GFP mRNA levels of the chimeric constructs compared with the WT constructs or chimeric constructs that contained a truncated sequence of the PTH mRNA element, and this effect was post-transcriptional. These results are in agreement with the decreased stability of the chimeric transcript in the *in vitro* degradation assay with PT proteins, and they demonstrate the functional importance of the RNA protein binding region in the PTH 3′-UTR (5). In order to understand the mechanism by which the specific sequences in the PTH mRNA 3′-UTR regulate mRNA half-life both *in vitro* and *in vivo* and PTH gene expression in response to changes in calcium and phosphate, we studied the structure of the PTH mRNA 3′-UTR. Our results show that the 3′-UTR and in particular the 100 nt that include the 26-nt protein binding core and flanking sequences do not form a stable secondary structure. Mutation analysis confirmed the importance of specific sequence patterns for protein binding and for the destabilizing effect of the *cis*-acting element.

MATERIALS AND METHODS

Construction of the chimeric GH and GFP mRNAs containing 63 and 100 nt, respectively, of the PTH mRNA 3′-UTR for transfection experiments. The 63- or 100-bp DNA corresponding to the PTH mRNA 3′-UTR 63- and 100-nt transcripts that were subcloned into PGEM-T vector (5) were excised. The 63-bp fragment or a 40-bp truncated fragment was inserted into the SmaI site of the pS16-GH expression plasmid that contained the S16 ribosomal protein promoter linked to the GH structural gene lacking GH promoter sequences (7). The 63- or 40-bp fragments were inserted between the coding region and the 3′-UTR of GH mRNA. For GFP chimeric constructs, a 100-bp fragment of the PTH mRNA 3′-UTR consisting of the 63-bp element and flanking nucleotides in pCRII plasmid (Invitrogen) was inserted into the SacI-ApaI site of the MCS of pEGFP-C1 (Clontech) at the 3′-end of GFP cDNA before the poly(A) signal. The mutated PTH 100-nt sequence was prepared by PCR using mutated oligonucleotides for each construct, as described below.

Transient Transfection Experiments—The plasmids (1 μg of DNA/24-well plate) were transiently transfected into HEK293 (human embryonic kidney) cells by calcium phosphate precipitation. In experiments using sense (oligonucleotide 1) or antisense (oligonucleotide 2) oligonucleotides, the oligonucleotides to the 26-nt protein-binding region were cotransfected at a concentration of 0.25 μg/well using LipofectAMINE (Invitrogen) according to the manufacturer's instructions. 24–48 h after transfection, total RNA was extracted by TRI reagent (Molecular Research Center, Cincinnati, OH) and analyzed for GH or GFP mRNAs by Northern blot. Expression of co-transfected cytomegalovirus-β-galactosidase plasmid demonstrated transfection efficiency. In some experiments, DRB (Sigma) (25 μg/ml) or actinomycin D (Sigma) (2.5 μg/ml) was added 24 h after transfection to suppress transcription for 3–24 h.

In Vitro RNA Synthesis—In vitro transcribed RNA was prepared from linearized plasmids using an RNA production kit (Promega) and the appropriate RNA polymerases as previously described (5). The RNAs were quantified by spectrophotometry at 260/280 and visualization on agarose gels.

RNase H Analysis—RNase H analysis was performed according to Argaman *et al.* (8) with some modifications. 3 pmol of oligonucleotides were annealed with 1 pmol of *in vitro* transcribed RNA by incubation at 37–45 °C according to the denaturing temperature of each oligonucleotide for 10 min in 10 mM HEPES, 3 mM $MgCl_2$, 40 mM KCl, 5% glycerol, and 1 mM dithiothreitol. Then $MgCl_2$ (10 mM) and 1 unit of RNase H (Promega) were added, and the samples were incubated at 37 °C for 30 min. The RNA samples were then extracted with phenol/chloroform, denatured, separated on 2% agarose gel, and transferred to Hybond N membrane. The membranes were hybridized for PTH and autoradiographed for 14 min. To analyze endogenous PT RNA, rat thyro/parathyroid RNA from a single rat was extracted with TRi reagent (Molecular Research Center) and subjected to RNase H analysis. For endogenous PTH mRNA, 9 pmol of oligonucleotide were annealed with 2 μg of total PT RNA, subjected to RNase H and analyzed as the *in vitro* transcribed RNA.

The oligonucleotides used were as follows from 5′ to 3′: the sense oligonucleotide 1 (CAATATATTCTTCTTTTTAAAGTATTA; residues 623–648) and the antisense oligonucleotides oligonucleotide 2 (TAATACTTTAAAAAGAAGAATATATTG; residues 648–623), oligonucleotide 3 (AAAGAAGAATATATTG; residues 638–623), oligonucleotide 4 (GGTTCATGA; residues 701–693), oligonucleotide 5 (TTTATTTATATTTAAGGAGAG; residues 684–663), oligonucleotide 6 (AAATGGAATCATTGGAAGAGAC; residues 622–601), oligonucleotide 7 (ATTACAGTAGAA; residues 562–551), oligonucleotide 8 (TCTAGAATACGT; residues 484–473), and oligonucleotide 9 (ATCATCACCTTA; residues 142–150). For the endogenous PT RNA, oligonucleotide dT consisting of 21 repeats was used. For the analysis of the chimeric GFP-PTH 100 transcript, the antisense oligonucleotide of the polylinker sequence of the pCRII plasmid that was also part of the GFP-PTH chimeric transcript was AAGTCCGGACTCAGATCTCGA.

PTH RNA Structure by Primer Extension—In vitro transcribed RNA for the full-length PTH mRNA, the 3′-UTR, or the 100 nt of the 3′-UTR (2 pmol) was partially digested by RNase T_1 and U_2 (Amersham Biosciences) and V_1 (Pierce). RNase T_1 digestion was performed at 37 °C for 10 min with 0.005–0.5 units of T1 in 20 mM Tris-HCl (pH 7.5), 100 mM NaCl, 0.5 mM $MgCl_2$, and 10 μg of tRNA. Digestion with U_2 was performed at 55 °C for 10 min with 0.005–0.5 units in 33 mM sodium citrate (pH 3.5), 1.7 mM EDTA, and 3.5 M urea. RNase V1 digestion was at 37 °C for 30 min with 0.01–0.4 units in 25 mM Tris, pH 7.5, 200 mM NaCl, 10 mM $MgCl_2$ and 10 μg of tRNA. All digestions were performed in a final volume of 10 μl. Reactions were stopped by phenol/chloroform extraction and precipitation with ethanol in the presence of 0.5 M NaCl and 1 μl of Quik-Precip (Edge Biosystems). A primer extension reaction was performed using a ^{32}P-5′-end-labeled antisense oligonucleotide complementary to the 3′-end of the PTH mRNA (antisense oligonucleotide 4 in Fig. 2*A*). An annealing mixture containing 2 pmol of 5′-end-labeled primer and 2 pmol of partially digested PTH RNA was incubated at 65 °C for 3 min and cooled at 4 °C for 15 min. Subsequently, the primer was extended toward the cleavage site by reverse transcription with 2 units of avian myeloblastosis virus reverse transcriptase (Promega) and 0.5 mM each dXTP for 20 min at 42 °C. The extension products were run on 6% sequencing gels along with a sequencing reaction that was carried out with the same end-labeled PTH primer. The sequencing reaction was performed using a Termo-sequenase kit (U.S. Biochemical Corp.). The gels were exposed to x-ray film.

Mutations for Binding and Transfection Experiments—The transcripts of WT and mutated 26-nt element (Fig. 4*A*) were prepared from annealed sense and antisense oligonucleotides that were constructed to include the T3 RNA polymerase sequence (underlined). For the WT 26 nt, the sense oligonucleotide was AATTAACCCTCACTAAAGGGCAATATATTCTTCTTTTTAAAGTATTAT, and the antisense oligonucleotide was TAATACTTTAAAAAGAAGAATATATTG. The mutations described in the legend to Fig. 4*B* were constructed by replacing two or three specific nt at a time, as indicated. The following sense oligonucleotides were used for the mutated transcripts: for m1, CAATATATTCTTCTTTTTAAAG**CCC**T; for m2, CAATATATTCTTCTTTTT**CC**AGTATT; for m3, CAATATATTCTTCT**GCG**TAAAGTATT; for m4, CAATATATTC**GG**CTTTTTAAAGTATT; for m5, CAATATA**CC**CTTCTTTTTAAAGTATT; for m6, C**CGC**ATATTCTTCTTTTTAAAGTATT. All oligonucleotides were linked to the T3 RNA polymerase sequence (not shown) as for the WT and annealed to the corresponding antisense oligonucleotides (not shown).

The mutated PTH 100-nt sequence was prepared by PCR using mutated oligonucleotides for each construct as shown in Fig. 4 and the antisense oligonucleotide 4 that is described for RNase H analysis. The PCR products were subcloned first into pGEM-T Easy vector (Promega) and then excised and inserted into the GFP expression plasmid as for the WT PTH 100-nt element.

Computer Analysis—The computer programs EDscan (9, 10) and SigStb (11–13) were used to search for well ordered folding patterns and/or unusual folding regions in the PTH mRNA. The program EDscan computed a standard Z score, $Zscr_e$ of the free energy difference, E_{diff} between the lowest free energy structure of the local segment and its corresponding optimal restrained structure where all base pairs formed in the original minimal structure were prohibited. The greater the E_{diff} of the segment is, the more well ordered the folded RNA structure is expected to be. Thus, the measures E_{diff} and $Zscr_e$ signify both the thermodynamic stability and well ordered conformation of a local folded segment. In practice, E_{diff} and $Zscr_e$ were computed by sliding a fixed length window in steps of one or a few nt from 5′ to 3′ along the sequence.

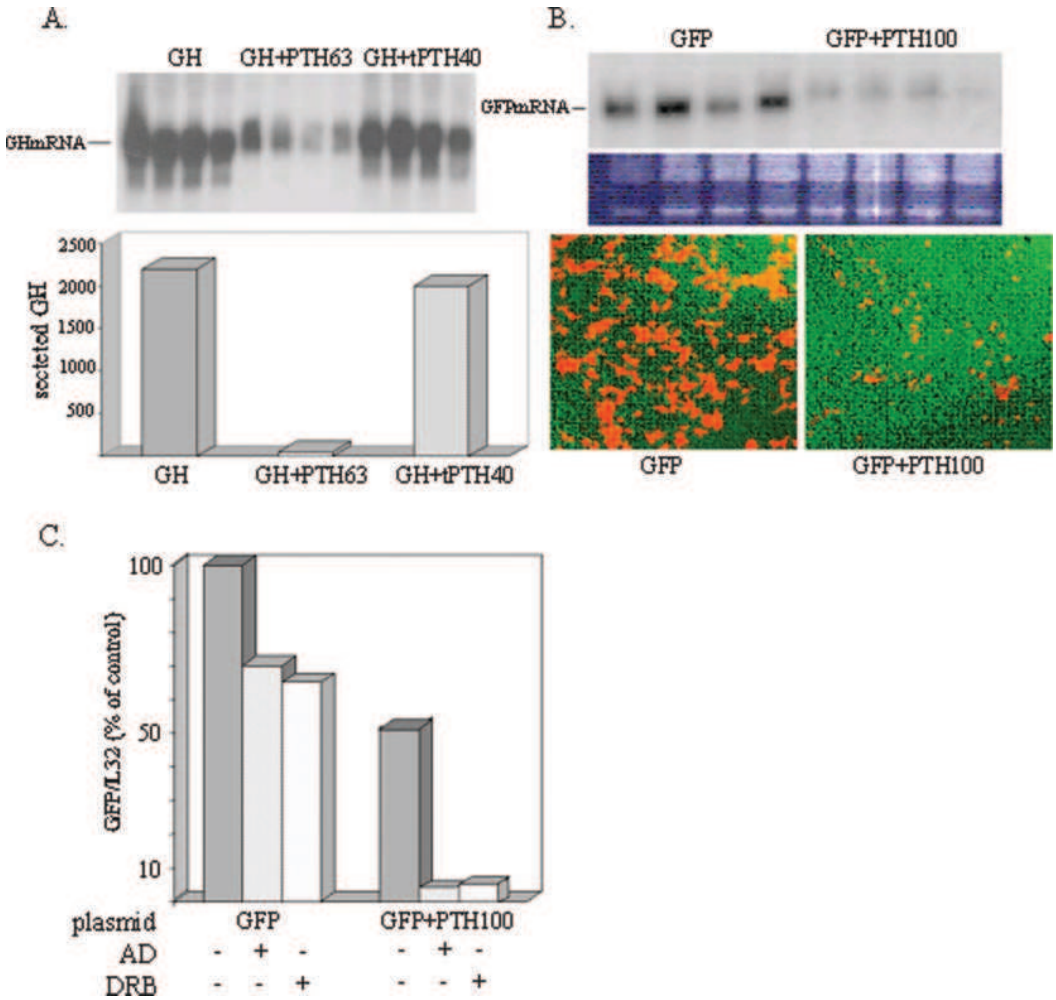

FIG. 1. **The PTH mRNA 3′-UTR *cis*-acting element decreases GFP and GH reporter gene mRNA and protein levels.** *A*, representative Northern blot for GH mRNA levels (*top*) and graph for the amount of GH protein secreted to the medium (*bottom*) of HEK293 cells that were transiently transfected with expression plasmids for WT GH (*GH*) or chimeric GH containing the PTH mRNA 3′-UTR 63-nt *cis*-acting element (*GH+PTH63*) or a truncated 40-nt element (*GH+tPTH40*). The gels show four separate transfections for each expression plasmid. *B*, representative Northern blot (*top*) for GFP mRNA levels of HEK293 cells that were transiently transfected in quadruplicate, with expression plasmids for WT GFP or chimeric GFP containing the PTH mRNA 3′-UTR 100-nt *cis*-acting element (*GFP+PTH100*). The *bottom panel* shows the expression of GFP protein by immunofluorescence. *C*, GFP mRNA levels are shown as percentages of L32 ribosomal mRNA levels in HEK 293 cells transiently transfected with the WT or chimeric GFP expression plasmids that were treated with actinomycin D (*AD*) or DRB for 16 h. The results of three independent experiments (four transfections for each treatment) are shown as percentages of mRNA levels in cells transfected with the WT GFP plasmid. Insertion of the mRNA 3′-UTR 63-nt *cis*-acting element into reporter mRNAs destabilized the mRNAs of both reporter genes.

The stability and statistical significance of a given RNA folding relative to others in the sequence were assessed by the two standard Z scores, significance score (SIGSCR) and stability score (STBSCR) (12, 13). The score SIGSCR of a local RNA segment was calculated by dividing the energy difference between the actual and mean random stabilities by the S.D. value of the random stabilities. The STBSCR was calculated by dividing the difference between the stability of the given segment and the mean stability of all overlapping segments by the S.D. value of the stabilities of these segments that were generated by taking successive, overlapping, fixed length segments stepped one or few nt at a time along the sequence. The primary approach SigStb was used to explore unusual folding regions whose SIGSCR and/or STBSCR are unusually small or large in the sequence by sliding a fixed length window along the sequence. The significant open region (14), whose SIGSCR and STBSCR are unusually large can be discovered. The term "significant open region" indicates that the structure folded by the biological segment is very unstable, and the structure of the random permutation of the biological sequences is statistically more stable than that of the natural sequence. The detailed instruction and online server of RNA2D (including EDscan and SigStb) are available on the World Wide Web at protein3d.ncifcrf.gov/shuyun/rna2d.html.

RESULTS

The Effect of the PTH mRNA 3′-UTR cis-Element on the Expression of Reporter Genes in HEK293 Cells—We have previously identified a protein-binding *cis*-acting element in the PTH mRNA 3′-UTR. We demonstrated the function of a 63-nt element in an IVDA with parathyroid cytosolic proteins and the PTH mRNA transcript or a chimeric reporter gene transcript containing the PTH element (5). To show the functionality of the *cis*-element *in vivo* in cells, we studied its effect on reporter genes by transfection experiments. Since there is no PT cell line, we studied the function of the PTH binding element in the heterologous cell line HEK293. We used plasmids containing the native GH gene or the chimeric GH PTH 63- or 40-nt truncated element all driven by a S16 ribosomal protein promoter. The truncated 40-nt element that was shown not to bind PT proteins was used as a control (5). The 63- or 40-bp fragments were inserted into the same site of a GH expression plasmid, between the coding region and the 3′-UTR of GH mRNA. The plasmids were transiently transfected into HEK293 cells, and mRNA levels were measured at 24 and 48 h by Northern blot. Fig. 1*A* shows a representative Northern blot for GH mRNA for four transfections of each expression plasmid. There was a marked decrease in GH mRNA levels of the GH PTH 63-nt chimeric construct but not of the truncated

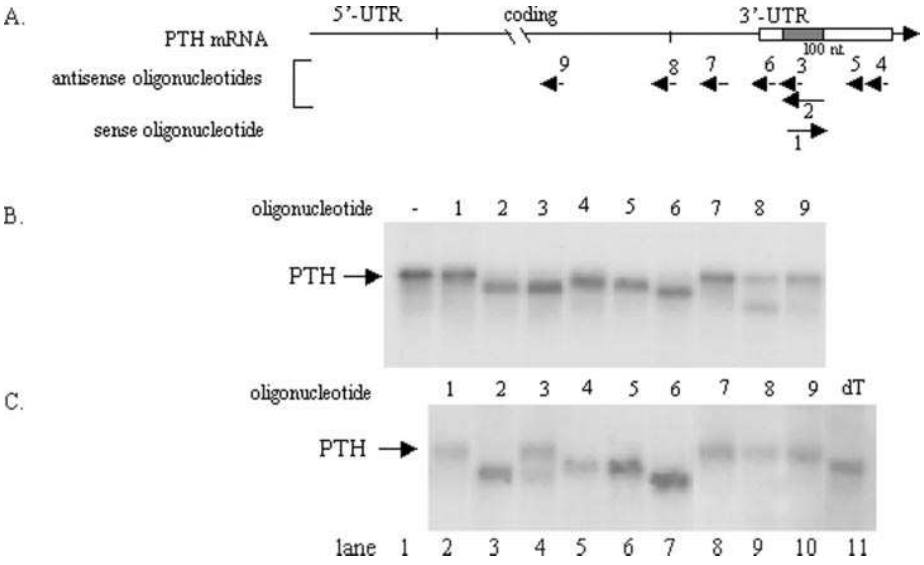

FIG. 2. **RNase H analysis of the PTH RNA shows that its 3′-UTR is mainly unstructured.** *A*, schematic representation of the PTH mRNA showing the coding and 5′- and 3′-UTRs and the sense oligonucleotide 1 and the antisense oligonucleotides 2–9 used for RNase H analysis. The 100-nt element in the PTH mRNA 3′-UTR is shown in an *open box*, and the 26-nt minimal binding element in the *hatched box*. *B*, Northern blot of *in vitro* transcribed full-length PTH RNA after incubation without (−) or with the indicated oligonucleotides and digestion with RNase H. *C*, Northern blot for PTH mRNA after incubation of total PT RNA with oligonucleotides 1–9 or oligonucleotide dT (*dT*) and RNase H digestion. The *lane numbers* are shown at the *bottom* of the gel.

40-nt construct compared with the WT GH construct at 24 h (not shown) or 48 h (Fig. 1*A*). Uniform transfection efficiency was demonstrated by cotransfection with a β-galactosidase expression plasmid. There was a similar decrease in secreted GH levels in the cell culture medium, shown as the mean for four transfections in each group (Fig. 1*A*). Because all GH constructs utilize the same S16 promoter, these results suggest that insertion of the 63-nt element decreased the stability of the GH transcript and not its transcription. These results are in agreement with the decreased stability of the GH chimeric transcript in the IVDA with PT proteins (5). These experiments demonstrate the functional importance of the RNA protein binding region in the PTH 3′-UTR as an instability element not only *in vitro* in the IVDA but also *in vivo* in HEK293 cells. To show the functionality of the *cis*-element in the context of another RNA, we used the cDNA for bacterial GFP as a reporter gene. A fragment coding for the PTH 3′-UTR 100 nt that included the 63 nt and flanking nt was inserted into a cytomegalovirus promoter-driven GFP plasmid at the 3′-end of the GFP cDNA before the polyadenylation signal. Wild type and chimeric plasmids were transiently transfected in quadruplicate into HEK293 cells. After 24 and 48 h, the expression of GFP protein was visualized by immunofluorescence, and then total RNA was extracted, and GFP mRNA levels were measured by Northern blot. Insertion of the PTH element resulted in a marked decrease in GFP mRNA and protein levels in the chimeric gene compared with the WT gene in the four transfections in each group (Fig. 1*B*). As for the GH mRNAs, this result suggests that the PTH element affected GFP mRNA stability and not its transcription, since both GFP constructs utilized the same cytomegalovirus promoter. To confirm the post-transcriptional effect of the PTH instability element, actinomycin D or DRB were added to the GFP-transfected cells 24 h after transfection. WT and chimeric GFP mRNA levels were measured by Northern blot at 16 h after the addition of the transcription inhibitors to compare the decay of the two mRNAs (Fig. 1*C*). The basal levels of wild type GFP mRNA levels before the addition of the transcriptional inhibitors (control) were set as 100%, and L32 was used as a control mRNA. The results are expressed as percentage of GFP/L32 mRNA levels and are the mean of three independent experiments each comprising four repeat samples. The presence of the 100-nt element decreased basal GFP mRNA levels by 50% (Fig. 1*C*) as in Fig. 1*B*. After transcriptional inhibition by the addition of DRB or actinomycin D, GFP WT mRNA levels decreased to 70% of base line at 16 h. In contrast, the mRNA levels for GFP with the 100-nt PTH element were decreased to 5% of basal level (Fig. 1*C*). This demonstrates that the GFP mRNA with the 100-nt PTH element was significantly less stable than the WT GFP mRNA. Therefore, the PTH mRNA 3′-UTR 100-nt element is a destabilizing element, and its effect is post-transcriptional.

Secondary Structure of the PTH mRNA—To understand how the PTH mRNA 3′-UTR 63 and 100 nt that include the protein-binding element destabilize the PTH transcript as well as reporter RNA, we analyzed the putative structure of the element. We first used oligonucleotide-targeted RNase H digestion to study the domain structure of the PTH transcript. RNase H cleaves DNA/RNA hybrids, and we used antisense oligonucleotides spanning different regions of the PTH mRNA and RNase H digestion to study the secondary structure of the PTH transcript. Targeted sequences that are part of a stable double-stranded structure will not anneal to the oligonucleotide and will therefore not be cleaved by RNase H. In contrast, antisense oligonucleotides will anneal to open regions in the transcript and will therefore mediate cleavage by RNase H. *In vitro* transcribed PTH RNA representing the full-length PTH mRNA or endogenous PTH mRNA as part of total parathyroid RNA extracted from rat parathyroids was used. We targeted sequences along the PTH 3′-UTR and coding region, using 6–20-nt-long antisense oligonucleotides (Fig. 2*A*). The antisense oligonucleotides were incubated with the RNA, and then RNase H was added. After digestion, RNA was extracted and analyzed by Northern blots. Fig. 2 shows the results of representative gels of RNase H analysis using a full-length *in vitro* transcribed RNA (Fig. 2*B*) and PTH mRNA of total parathyroid RNA (Fig. 2*C*). The RNAs were incubated with oligonucleotide 1 in the sense orientation that does not anneal to the RNA or oligonucleotides 2–9 in the antisense orientation (Fig. 2*A*). As expected, the full-length *in vitro* transcribed PTH transcript without added oligonucleotides (Fig. 1*B*, *first lane*) or with oligonucleotide 1 in the sense orientation (Fig. 1*B*, *lane 2*) was not cleaved by RNase H. In addition, antisense oligonucleotides 7 and 9 did not mediate cleavage of the RNA, suggesting that they target sequences that are double-stranded. Oligonucleotide 8 showed partial cleavage, suggesting that the target of this oligonucleotide is only partly double-stranded. In contrast, the addition of antisense oligonucleotides 2–6 spanning the 100-nt element all led to complete cleavage of the PTH RNA. Cleavage by RNase H resulted in two fragments. The larger 5′

cleavage product is seen in Fig. 2*B*, and the smaller 3′ corresponding cleavage product was seen after longer exposure of the gels (not shown). The size of the cleavage product was proportional to the distance of the oligonucleotide used from the 5′-end of the transcript. RNase H cleavage with oligonucleotide 4, which is close to the 3′-end of the transcript, resulted in a small decrease in the size of the full-length transcript (Fig. 2*B*, *lane 5*). In contrast, oligonucleotide 6, which is more proximal, mediated cleavage that resulted in a smaller 5′ transcript than with oligonucleotide 4 (Fig. 2*B*, *lane 7*) RNase H cleavage is dependent upon annealing of the antisense oligonucleotide to a single-stranded accessible region in the target RNA. When the antisense oligonucleotides were added to the PTH transcript that had been previously denatured by heating at 80 °C, there was cleavage by RNase H with all of the oligonucleotides, including oligonucleotides 7 and 9 (not shown). This confirms that in the undenatured RNA, secondary structures had prevented annealing to the regions targeted by these oligonucleotides. Fig. 2*B* shows the results of *in vitro* transcribed PTH RNA. Similar results were obtained when the same experiments were performed on endogenous PTH mRNA that had been transcribed and processed *in vivo* in the rat parathyroid (Fig. 2*C*). For that, RNase H analysis was performed as in Fig. 2*B* but with total RNA extracted from the rat parathyroid (Fig. 2*C*). The only significant difference was seen with oligonucleotide 8 (*lane 9*) that showed no cleavage with the endogenous PTH mRNA and partial cleavage with the *in vitro* transcribed RNA. The reason for this is not clear, but oligonucleotide 8 targets RNA that is not part of the 3′-UTR; therefore, its exact structure is less relevant to this study. The RNase H cleavage analysis shows that the results obtained with the *in vitro* transcribed RNA are relevant for the PTH mRNA that was transcribed and processed *in vivo*. The fact that antisense oligonucleotides 7 and 9 did not mediate cleavage by RNase H suggests that the coding region and the 5′- part of the 3′-UTR are more structured. In contrast, RNase H cleavage of the 100-nt element mediated by antisense oligonucleotides 2–6 suggests that this is an open region in the PTH mRNA and that at least major segments of this region do not have a stable double-stranded structure.

The 100-nt element of the PTH mRNA decreased the stability of the GFP mRNA in transfection experiments in HEK293 cells (Fig. 1). If the open structure of the PTH mRNA 100-nt element is important for its function to regulate mRNA stability of PTH and reporter genes, we would expect that it remains as an unstructured region also in the GFP mRNA. We therefore studied the structure of the 100 nt of the PTH mRNA 3′-UTR in the GFP RNA. *In vitro* transcribed chimeric GFP transcripts containing the PTH 100-nt element were analyzed by RNase H with antisense oligonucleotides 2, 3, 5, and 6 spanning the PTH 100-nt element (not shown). The antisense oligonucleotides for the PTH element mediated cleavage, but the sense oligonucleotide 1 and antisense oligonucleotide for the polylinker sequence of the pCRII plasmid that was also part of the chimeric transcript did not mediate cleavage (not shown). These results show that the same antisense oligonucleotides that mediated cleavage of the 100 nt in the full-length PTH transcript also mediated cleavage in the 100-nt PTH element within the chimeric GFP transcript. Therefore, the 100-nt element has an open structure in both PTH mRNA as well as when inserted into the GFP reporter gene. The open structure may be important for the function of this element.

RNase H can only give an estimation of the domain structure of the RNA because of the fact that RNase H cleaves RNA/DNA hybrids of 6–8 nt and cannot give information on the structure of specific nucleotides (15). To determine the structure of the PTH mRNA in greater detail, we performed primer extension experiments to identify the pairing of specific nt.

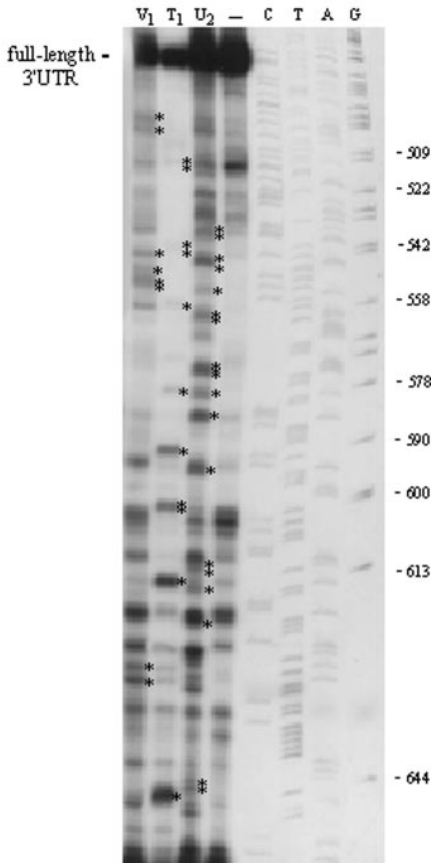

FIG. 3. **Primer extension analysis of the PTH mRNA 3′-UTR using structure-sensitive RNases suggests that the PTH mRNA 3′-UTR has an open structure.** *In vitro* transcribed RNA for the PTH mRNA 3′-UTR was subjected to partial cleavage with V1 (cleaves double-stranded RNA), T1 (cleaves ssGpN), and U2 (cleaves ssApN) or no cleavage (−) and then reverse transcribed using oligonucleotide 4 of Fig. 1. The cDNAs were separated on a sequencing gel along with a sequencing reaction for the PTH mRNA 3′-UTR cDNA fragment using the same oligonucleotide. *, cleavage sites that are above background as shown in the *fourth lane* (−). The locations of the G nt of the sequencing reaction are enumerated to the *right* of the gel. The full-length reverse transcribed 3′-UTR cDNA is indicated to the *left* of the gel. The full-length 3′-UTR is from 466 to 704 of the PTH cDNA. The 63-nt functional element is from 600 to 663, and the 26-nt core element is from 623 to 648. There was digestion of the RNA at most of the sites by the enzymes that cut single-stranded RNA but very little cleavage by RNase V1 that cuts double-stranded RNA.

Primer Extension Analysis of the PTH mRNA—More detailed information regarding PTH mRNA structure was obtained by primer extension analysis of PTH transcripts that were partially cleaved by structure-specific RNases (8). Transcripts for the full-length PTH, the 3′-UTR, and the 100-nt functional region were partially cleaved by RNase T_1 (specific for single-stranded guanine residues), RNase U_2 (specific for single-stranded adenine residues), or RNase V_1 (specific for double-stranded regions). To map the cleavage sites, the partially cleaved transcripts were subjected to primer extension with a ^{32}P-end-labeled antisense primer to the 3′-end of the PTH transcript (oligonucleotide 4 in Fig. 2*A*). The resulting cDNA products were analyzed by sequencing gel electrophoresis. The results of a representative sequencing gel for the PTH mRNA 3′-UTR transcript are shown in Fig. 3. Without cleavage, primer extension of the *in vitro* transcribed PTH 3′-UTR resulted in a major band representing the full-length cDNA and additional laddering of smaller fragments. These frag-

ments may represent either secondary structure of the RNA with resultant stop signals or, more likely, termination signals for T3 RNA polymerase that was used to transcribe the PTH RNA. There are two types of terminators for T3/T7 polymerase that are known to cause pausing and/or termination by these polymerases (16). Class I encodes RNAs that form stable stem loop structures followed by a run of U residues. Class II was in fact first identified in the cloned human PTH gene (16, 17, 19). These signals share a common sequence rather than a structural motif. Computer search of the rat PTH cDNA identified 15 potential T3/T7 terminators, six of which are in the 3′-UTR. It is therefore reasonable to conclude that the ladder of primer extension products is a result of partial transcript termination *in vitro* of the analyzed RNA. The interpretation of the primer extension of the structure-sensitive RNases was therefore analyzed above the background of the untreated RNA.

There was more cleavage of the PTH mRNA 3′-UTR by the enzymes that cleave single-stranded RNA at most of the nucleotides relevant for each of the enzymes: U_2 (ssApN), and T_1 (ssGpN) (Fig. 3). RNase V_1, which only cuts double-stranded RNA, produced very little cleavage and even less toward the 3′-end. Similar results were obtained when the primer extension was performed with the full-length 700-nt PTH transcript and with a transcript for the functional 100 nt of the PTH mRNA 3′-UTR (not shown). Analysis of 5′-end labeled PTH RNA directly after partial digestion by these enzymes was not more informative than the primer extension (not shown), probably because of premature termination of the T3/T7 transcribed RNA. The primer extension analysis is supportive of an open structure for most of the regions of the PTH mRNA 3′-UTR and more so for its 3′ terminal part.

Computer-assisted Structural Analysis of the PTH mRNA 3′-UTR—The structural feature of rat PTH mRNA was first explored by the program EDscan. In the calculation, we used a set of windows from 30 to 300 nt by a step of 5 nt and from 300 to 410 nt by a step of 10 nt. For each fixed length window, $Zscr_e$ values were repeatedly computed by moving the windows in steps of 3 nt from 5′ to 3′ along the PTH mRNA. Our results indicate that no distinct well ordered folding patterns are found in the 3′-UTR of rat PTH.

The extensive search by EDscan demonstrates that there is no well ordered RNA secondary structures that are both thermodynamically stable and uniquely folded in the 3′-UTR. However, we detected significant open regions in the 3′-UTR of rat PTH using the program SigStb. In the computation of SIGSCR and STBSCR, we slid the two fixed-length windows of 100 and 63 nt in steps of 1 nt at a time along the PTH mRNA. Our results show that the significant open regions dominate in the 3′-UTR. For rat PTH, we discovered nine open regions whose SIGSCR was >1.0 and STBSCR was >2.1 by the 100-nt window. They are all located at the 3′-UTR, and the most significant open region is segment 600–699, whose SIGSCR was 1.4 and whose STBSCR was 2.2. We also found eight open regions by sliding the 63-nt window. They are also located at the 3′-UTR, and the most significant open region is located at 625–687, whose SIGSCR was 1.4 and whose STBSCR was 2.1. Our results show that the folded structure in the 3′-UTR of rat PTH is not only much less stable than those of the coding region but also less stable than those from randomly shuffled sequences. The detected significant open regions include the 26-nt conserved sequence.

We repeated our search for those open regions in the PTH mRNAs of humans, cats, dogs, and mice with the same parameters as used in the rat PTH by SigStb. Our results show that the detected open regions dominate in the 3′-UTR of these PTH mRNAs. For the 100-nt window, the most significant open regions are regions 565–664, 554–653, 537–636, and 633–732 in humans, cats, dogs, and mice, respectively. These significant open regions include the corresponding 26-nt conserved sequence in these PTH mRNAs (Fig. 4*A*). Our results strongly suggest that there are no distinct well ordered folding patterns in the PTH mRNA 3′-UTR, and the 3′-UTRs of PTH mRNAs are dominated by statistically significant, open regions or nonhelical regions of the RNA structure.

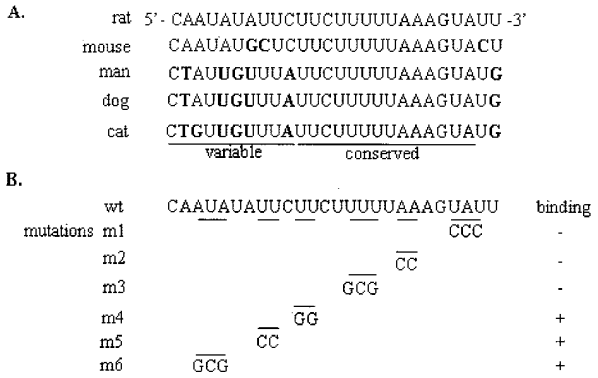

FIG. 4. **Identification of the homologous sequences of the rat PTH mRNA 3′-UTR 26-nt protein-binding element in mice, humans, cats, and dogs.** *A*, sequence alignment of the rat 26-nt element in mouse, human, dog, and cat PTH mRNA 3′-UTRs. The nt that are not conserved are shown in *boldface type*. The element was divided into two regions according to the similarity of the sequences. The first 10 nt are more variable than the stretch of 14 nt that are conserved in all species. *B*, the rat PTH mRNA 3′-UTR 26-nt element and mutations that were constructed to study their effect on protein-RNA binding and on the destabilizing function of the PTH mRNA 3′-UTR 26-nt region. Mutations 1–6 were created by replacing 2 or 3 nt at a time in the template DNA for the 26-nt transcript, as indicated. Shown on the *right* is a summary of the results of binding of PT protein extracts to RNAs that were transcribed from the mutated oligonucleotides as shown in Fig 5*A*. +, positive binding by REMSA; −, no binding. The accession numbers for the PTH sequences are as follows: rat, XO5721; mouse, AF066075; human, V00597; dog, U15662; cat, AF309967.

The Effect of Specific Mutation in the PTH cis-Element on Protein Binding and RNA Stability—Our results indicate that the PTH mRNA 3′-UTR does not have a stable secondary structure, at least in the absence of proteins. To study the role of specific nt in the *cis*-element in determining RNA stability, we constructed mutations in specific nucleotides of the *cis*-acting element and determined their effect upon binding and function. We have previously shown by binding experiments that the core 26-nt sequence in the 63-nt *cis*-acting element of the PTH mRNA 3′-UTR is sufficient for protein-RNA binding (5). The 26-nt element was also identified by sequence alignment of PTH mRNAs of different species (Fig. 4*A*). Comparison of the sequence of the 26-nt element of humans, rats, mice, dogs, and cats distinguishes between a variable region from nt 623 to 633 of the rat PTH mRNA and a highly conserved stretch of 14 nt from 634–648. We created mutations of specific nt in both regions of the 26-nt sequence and studied their effect on protein binding (Fig. 5*A*). We also studied their function as a destabilizing element within the 100-nt 3′-UTR element on GFP expression in transfected cells (Fig. 5*B*).

Two or three nt were mutated each time in the template DNA for the 26-nt transcript as shown in Fig. 4*B*, and RNA was transcribed. The wild type and mutated transcripts were analyzed for binding to PT cytosolic proteins by REMSA (Fig. 5*A*). Mutations in the conserved region (mutations 1, 2, and 3 in Fig. 4*B*) resulted in no binding of PT proteins (Fig. 5*A*). In contrast, mutated transcripts in the more variable region (mutations 4–6 in Fig. 4*B*) did not affect binding. These results show that the specific nt sequence in the conserved region of the 26-nt PTH mRNA 3′-UTR is essential for protein-RNA binding.

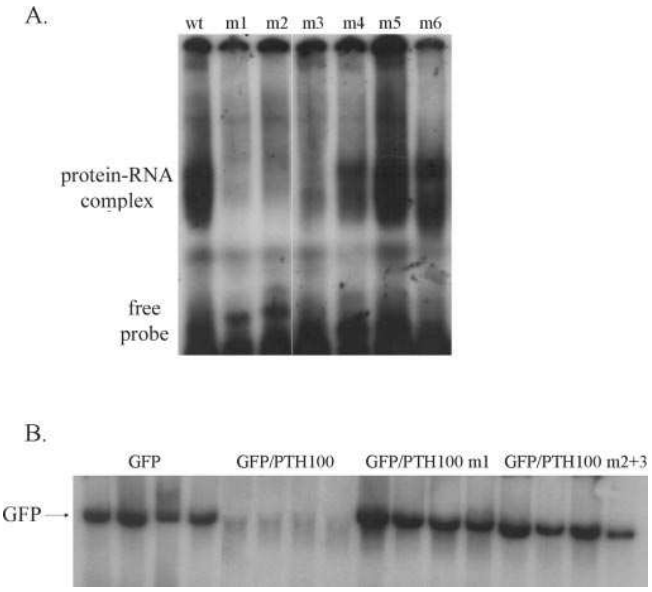

FIG. 5. **Mutation in the phylogenetically conserved part of the PTH mRNA 3′-UTR 26-nt protein-binding element but not in the more variable part disrupted protein binding and prevented the degradation of reporter GFP mRNA in transfected HEK293 cells.** *A*, representative REMSA for the binding of PT cytosolic protein extracts to transcripts for the WT PTH mRNA 3′-UTR 26-nt element or mutated transcripts shown in Fig. 4*B*. The free probe and the shifted protein-RNA complex are shown. *B*, Northern blot for GFP mRNA levels in HEK293 cells that were transiently transfected with WT or chimeric GFP expression plasmids that contained the native PTH mRNA 3′-UTR 100-nt element or the 100-nt element containing mutation 1 or mutations 2 and 3 together in the 26-nt element shown in Fig. 4*B*. Cotransfection with cytomegalovirus β-galactosidase expression plasmid showed that there was no difference in transfection efficiency using the different GFP constructs.

To study the effect of selected mutations on the functionality of the PTH mRNA 3′-UTR 100 nt, we mutated specific nt in the conserved region of the 26-nt element, within the PTH mRNA 3′-UTR 100 nt, and inserted the 100 nt into the expression plasmid for GFP as before. The plasmids were transiently transfected into HEK293 cells, four transfections in each group, and their effect on GFP mRNA levels was determined as in Fig. 1. The mutations used in each experiment are indicated in Fig. 5*B*. Insertion of the PTH mRNA 3′-UTR 100-nt WT sequence resulted in a decrease in GFP mRNA levels (Fig. 5) as before (Fig. 1*B*). Mutations in the conserved region of the PTH mRNA 3′-UTR 26-nt core binding element within the 100 nt abolished the destabilizing effect of the PTH mRNA 3′-UTR 100 nt (Fig. 5*B*, *m1* and *m2+3*). This region was mutated in two discrete sets of nt of the PTH mRNA, and all of them lost their destabilizing function. The results shown are representative of three repeat experiments. In binding assays, mutating these nt resulted in loss of protein binding to these transcripts (Fig. 5*A*). These results suggest that the nt sequence preserved in the conserved region of the 26 nt is important both for binding and for destabilization of the PTH mRNA.

To test whether the PTH element is also in an open structure *in vivo* in the cell where it is bound to proteins and polysomes, we used antisense oligonucleotides to the 26-nt element. We cotransfected the chimeric GH reporter gene containing the 63- or 40-nt truncated element of the PTH mRNA 3-UTR with a specific antisense oligonucleotide or sense oligonucleotide as control. The antisense oligonucleotide decreased GH mRNA levels compared with the sense transfected cells when the chimeric gene contained the full 63-nt element (Fig. 6). The truncated GH PTH 40-nt element mRNA levels were not affected by either oligonucleotide (Fig. 6).

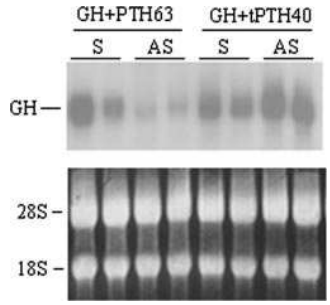

FIG. 6. **Antisense oligonucleotides to the PTH mRNA 3′-UTR element decreases a chimeric GH mRNA containing the functional 63-nt element but not a truncated 40-nt element.** HEK293 cells were transiently cotransfected in duplicate with a GH expression plasmid containing the 63-bp *cis*-acting element (*GH+PTH63*) or a truncated 40-bp element (*GH+tPTH40*) as a control and oligonucleotides to the 26-nt core element in sense (*S*) or antisense (*AS*) orientation. After 24 h, GH mRNA levels were analyzed by Northern blots (*top*). Ethidium bromide staining of the membrane showing the 28 and 8 S ribosomal RNA (*bottom*) shows equal RNA loading. This gel is representative of three separate experiments.

These results suggest that the antisense oligonucleotide anneals to the sequence in the 63-nt element of the chimeric transcript and thereby induces endogenous RNase H cleavage of the RNA-DNA hybrid (20). This effect is specific for the antisense, because the sense oligonucleotide had no effect, and a truncated 40-nt element in the GH mRNA was not a target to either oligonucleotide. These results support our structure analysis *in vitro* that the PTH mRNA 3′-UTR *cis*-acting element is an open structure.

DISCUSSION

We have developed a reporter assay for the function of the PTH mRNA 3′-UTR defined element. Using two reporter genes, GFP and GH, we have shown that the protein-binding element in the PTH mRNA 3′-UTR destabilizes the reporter mRNAs in HEK293 cells. This is in agreement with our results using an *in vitro* degradation assay of chimeric GH PTH mRNA 3′-UTR 63-nt and parathyroid cytosolic proteins. In the IVDA the PTH mRNA, 3′-UTR 63 nt destabilized the GH transcript and conferred responsiveness to parathyroid extracts from rats fed low calcium or low phosphate diets. The low calcium PT proteins stabilized and the low phosphate PT proteins destabilized the chimeric transcript compared with control, similar to the full-length PTH transcript (5). There is no PT cell line, and there is no other cell line that responds to changes in extracellular calcium and phosphate like the parathyroid does. However, our results show that HEK293 cells are able to reproduce the destabilizing effect of the PTH mRNA 3′-UTR element. RNA stability reflects the balance between stabilizing and destabilizing cytosolic factors that act on the transcribed mRNA. The PTH mRNA 3′-UTR-binding proteins that protect the RNA from degradation in the PT cytosol are ubiquitous, but only in the PT is their binding and function regulated by calcium and phosphate. In the HEK293 cell, there is a given amount of cytosolic binding protein that after transfection binds and prevents degradation mediated by the 100-nt destabilizing element. Excess chimeric GFP PTH mRNA 3′-UTR 100 nt saturates the protective binding proteins and results in the decrease in chimeric GFP mRNA levels but not of the native GFP that is not affected by these factors.

We used the GFP-PTH mRNA 3′-UTR 100-nt chimeric gene to determine the role of specific nt in destabilizing the reporter gene. We have previously shown that there is a conserved 26-nt core element in the PTH mRNA 3′-UTR that is sufficient for protein binding. This minimal binding element is conserved among humans, dogs, cats, rats, and mice compared with the

rest of the 3′-UTRs that are far less conserved. We mutated specific nt in the PTH mRNA 3′-UTR 26-nt core protein-binding element. We studied the effect of these mutations on binding of PT proteins to the mutated PTH transcript and their destabilizing function in the chimeric GFP gene. The mutated transcripts of the 26 nt that did not bind PT proteins in REMSA also did not destabilize the GFP mRNA in the transfected HEK293 cells. All of the mutations that disrupted the function and binding of the PTH mRNA 3′-UTR element were at the 3′-region of the 26-nt element and localized to 14 nt. These 14 nt were completely preserved within mouse, human, dog, and cat PTH mRNA 3′-UTR, suggesting that this sequence is of functional importance. The 5′-portion of the 26-nt core element is not as conserved among the species. Mutations in this less conserved region did not affect binding, suggesting that the sequence of this region may be of less functional significance. In addition, a transcript for the human 26-nt element bound human and rat parathyroid proteins with the same affinity as the rat element,[2] indicating that the 5 nt that differ in the variable region of the human PTH mRNA 26-nt element do not affect the binding of PT rat proteins.

mRNA stability and its translation may be determined by both sequence and structure of the RNA. A well defined example is the regulation by iron of ferritin translation and the transferrin receptor mRNA stability by a stem and loop iron-responsive element (21, 22). A stem loop structure is also involved in determining the stability of histone H4 mRNA. Interaction of this stem loop structure, located at the 3′-end of the mRNA with cellular proteins promotes degradation of the mRNA (23). The most widely spread family of instability sequences are the AREs that generally promote rapid degradation following deadenylation of the mRNA (24), although in the GROα mRNA, endonucleolytic cleavage within the ARE is the initial event in degradation of the mRNA (25). Chen *et al.* (26) have recently shown that the exosome is recruited by ARE-binding proteins that interact with the exosome that then promotes rapid degradation of ARE containing mRNAs.

Computer analysis as well as the results of the primer extension and RNase H analysis showed that the 3′-region of the PTH mRNA 3′-UTR has no stable structure. Mutation analysis also supports the importance of sequence rather than structure. This suggests that this RNA region is open, which is an unusual finding. The PTH mRNA 3′-UTR functional region is an AU-rich element that binds AUF1, which stabilizes the PTH transcript (6). However, it does not have the canonical AUUUA pentamer, which therefore classifies it as a type III ARE (24). The structure of the mRNAs that contain AREs has not yet been determined. It would be of interest to know whether there is a contribution of structure to the function of any of the other AREs in particular type III AREs. Wilson *et al.* (27) showed that magnesium-induced conformational changes in the ARE of tumor necrosis factor-α mRNA inhibited AUF1 binding. In addition, using resonance energy transfer to characterize structural changes in RNA substrates in response to cations and AUF binding, it was shown that association of AUF1 with an ARE may function to remodel local RNA structures that may be important for its function (18). The results presented here with the PTH mRNA 3′-UTR, showing that it is dominated by significant open regions, are the first to indicate that the ARE functions in regulating mRNA stability without having a defined structure. It is possible that in the presence of cellular RNA-binding proteins, the unstable structure of the free mRNA may adopt a more defined structure. We showed that an antisense oligonucleotide to the PTH mRNA 3′-UTR 26-nt element specifically decreased mRNA levels in transfected HEK293 cells. This is most likely due to annealing that induces degradation of the RNA by endogenous RNase H (20). The inference is that the target RNA is in a configuration that allows annealing of the oligonucleotide to its target. For this to happen, the target RNA is presumably open *in vivo* in the cell as it is *in vitro*. In any case, most of the assays for RNA regulation, such as protein-RNA binding, IVDA, *in vitro* translation, etc., utilize *in vitro* transcribed RNA. The fact that these assays reproduce the *in vivo* regulation of mRNA fate suggests that the structure that may be induced by the endogenous proteins is not essential for these *in vivo* processes that can be simulated *in vitro*. In particular, the regulation of PTH RNA binding and RNA stability by calcium and phosphate can be demonstrated with *in vitro* transcribed PTH RNA, suggesting that this regulation occurs with an open structured PTH mRNA 3′-UTR.

Acknowledgments—We thank Miriam Offner for skilled technical assistance, Oded Meyuhas for the S16 GH plasmid, and Shoshy Altuvia for helpful discussions.

[2] R. Kilav, O. Bell, S.-Y. Le, J. Silver, and T. Naveh-Many, unpublished observations.

REFERENCES

1. Silver, J., Naveh-Many, T., and Kronenberg, H. M. (2002) in *Principles of Bone Biology* (Bilezikian, J. B., Raisz, L. G., and Rodan, G. A., eds) pp. 407–420, Academic Press, Inc., San Diego
2. Moallem, E., Silver, J., Kilav, R., and Naveh-Many, T. (1998) *J. Biol. Chem.* **273,** 5253–5259
3. Kilav, R., Silver, J., and Naveh-Many, T. (1995) *J. Clin. Invest.* **96,** 327–333
4. Naveh-Many, T., Rahamimov, R., Livni, N., and Silver, J. (1995) *J. Clin. Invest.* **96,** 1786–1793
5. Kilav, R., Silver, J., and Naveh-Many, T. (2001) *J. Biol. Chem.* **276,** 8727–8733
6. Sela-Brown, A., Silver, J., Brewer, G., and Naveh-Many, T. (2000) *J. Biol. Chem.* **275,** 7424–7429
7. Levy, S., Avni, D., Hariharan, N., Perry, R. P., and Meyuhas, O. (1991) *Proc. Natl. Acad. Sci. U. S. A.* **88,** 3319–3323
8. Argaman, L., and Altuvia, S. (2000) *J. Mol. Biol.* **300,** 1101–1112
9. Le, S. Y., Chen, J. H., Konings, D., and Maizel, J. V. (2002) *Proceedings of the 2002 International Conference on Mathematics and Engineering Techniques in Medicine and Biological Sciences*, pp. 41–45, CSREA Press, Las Vegas, NV
10. Le, S. Y., Chen, J. H., Konings, D., and Maizel, J. V. (2003) *Bioinformatics* **10,** 354–361
11. Le, S. V., Chen, J. H., Currey, K. M., and Maizel, J. V., Jr. (1988) *Comput. Appl. Biosci.* **4,** 153–159
12. Le, S. Y., and Maizel, J. V., Jr. (1989) *J. Theor. Biol.* **138,** 495–510
13. Le, S. Y., Chen, J. H., and Maizel, J. V. (1990) in *Structure and Methods VI: Human Genome Initiative and DNA Recombination* (Sarma, R. H., and Sarma, M. H., eds) Adenine Press, Schenectady, NY
14. Le, S. Y., Chen, J. H., Chatterjee, D., and Maizel, J. V. (1989) *Nucleic Acids Res.* **17,** 3275–3288
15. Donis-Keller, H. (1979) *Nucleic Acids Res.* **7,** 179–192
16. Macdonald, L. E., Durbin, R. K., Dunn, J. J., and McAllister, W. T. (1994) *J. Mol. Biol.* **238,** 145–158
17. He, B., Kukarin, A., Temiakov, D., Chin-Bow, S. T., Lyakhov, D. L., Rong, M., Durbin, R. K., and McAllister, W. T. (1998) *J. Biol. Chem.* **273,** 18802–18811
18. Wilson, G. M., Sutphen, K., Moutafis, M., Sinha, S., and Brewer, G. (2001) *J. Biol. Chem.* **276,** 38400–38409
19. Mead, D. A., Szczesna-Skorupa, E., and Kemper, B. (1986) *Protein Eng.* **1,** 67–74
20. Toulme, J. J. (2001) *Nat. Biotechnol.* **19,** 17–18
21. Klausner, R. D., Rouault, T. R., and Harford, J. B. (1993) *Cell* **72,** 19–28
22. Theil, E. C., and Eisenstein, R. S. (2000) *J. Biol. Chem.* **275,** 40659–40662
23. Ross, J. (1995) *Microbiol. Rev.* **59,** 423–450
24. Chen, C. Y., and Shyu, A. B. (1995) *Trends Biochem. Sci.* **20,** 465–470
25. Stoeckle, M. Y. (1992) *Nucleic Acids Res.* **20,** 1123–1127
26. Chen, C. Y., Gherzi, R., Ong, S. E., Chan, E. L., Raijmakers, R., Pruijn, G. J., Stoecklin, G., Moroni, C., Mann, M., and Karin, M. (2001) *Cell* **107,** 451–464
27. Wilson, G. M., Sutphen, K., Chuang, K., and Brewer, G. (2001) *J. Biol. Chem.* **276,** 8695–8704